

Short communication

# Electrochemical properties of lithium sulfur cells using PEO polymer electrolytes prepared under three different mixing conditions

S.S. Jeong, Y.T. Lim, Y.J. Choi, G.B. Cho, K.W. Kim\*, H.J. Ahn, K.K. Cho

*Global Leader Development Center for i-cube Materials and Parts & ITRC for Energy Storage & Conversion,  
Gyeongsang National University, Jinju 660-701, South Korea*

Available online 27 June 2007

## Abstract

Lithium sulfur cells were prepared by composing with sulfur cathode (PEO)<sub>6</sub>LiBF<sub>4</sub> polymer electrolyte and lithium anode. (PEO)<sub>6</sub>LiBF<sub>4</sub> polymer electrolyte was prepared under three different mixing conditions: stirred polymer electrolyte (SPE), ball-milled polymer electrolyte (BPE) and ball-milled polymer electrolyte with 10 wt%Al<sub>2</sub>O<sub>3</sub> (BCPE). The effects of ball milling and additive were investigated by discharge test according to depth of discharge. The initial discharge capacity of lithium sulfur cell using BCPE was 1670 mAh g<sup>-1</sup>-sulfur, which was better than those of SPE and BPE, and approximately equal to the theoretical capacity. The cycle performance of Li/(PEO)<sub>6</sub>LiBF<sub>4</sub>/S cell was remarkably improved by the addition of Al<sub>2</sub>O<sub>3</sub>.

© 2007 Elsevier B.V. All rights reserved.

**Keywords:** Sulfur; Polymer electrolyte; Ball milling; Lithium sulfur cell; Al<sub>2</sub>O<sub>3</sub>

## 1. Introduction

Elemental sulfur is a very attractive cathode material for lithium batteries because sulfur is cheap and harmless. Lithium sulfur cell has a theoretical specific capacity of 1672 mAh g<sup>-1</sup>-sulfur and specific energy of 2600 Wh kg<sup>-1</sup>-sulfur, basing on the formation of Li<sub>2</sub>S. Unfortunately, lithium sulfur cells had not been sufficiently utilized in lithium secondary batteries with conventional liquid electrolyte because LiS<sub>n</sub> dissolved into liquid electrolyte. During the discharge process, sulfur react electrochemically with lithium to produce lithium polysulfides (LiS<sub>n</sub> such as Li<sub>2</sub>S<sub>8</sub>, Li<sub>2</sub>S<sub>4</sub>, Li<sub>2</sub>S<sub>2</sub>) and lithium sulfide (Li<sub>2</sub>S) [1]. In general, the discharge process of Li/S battery proceeds by two steps [1]. The first step is transformation of sulfur to LiS<sub>n</sub>, and LiS<sub>n</sub> dissolved into electrolytes. The second step is the change of LiS<sub>n</sub> to Li<sub>2</sub>S. This dissolution causes an irreversible loss at sulfur active material. To overcome this problem, various adsorption materials such as FW200 (Dequssa, Co.) Cabosil 530 (Cabot Co.), Crystalline Vanadium Oxide Aerogel have been suggested, and these adsorbing materials are very effective for improving cycle life [2]. How-

ever, the amount of active material in cathode electrode is decreased.

Dry polymer electrolytes, such as PEO-Li-salt complex, can be introduced to restrain the dissolution of polysulfides into the electrolyte. However, the linear PEO-Li-salt polymer electrolytes generally have some problems in lithium polymer battery. The problems are active reactivity of lithium anode at high temperature and low ionic conductivity at low temperature. Some researchers have been tried to overcome the problems by the use of ceramic filler such as Al<sub>2</sub>O<sub>3</sub>, SiO<sub>2</sub>, and TiO<sub>2</sub> in PEO based polymer electrolyte [3–5]. It was reported that the additive improved the conductivity of PEO-base electrolytes as well as their interfacial resistance between the electrolyte and the lithium electrode. Moreover, the additions of ceramic fillers are accompanied with amorphous PEO structure. The amorphous PEO electrolyte also improves ionic conductivity.

Another approach is to decrease the crystallinity of the polymer in order to improve the polymer chain mobility. Smith et al. [6] have reported that high energy mechanical milling conducted at ambient and cryogenic temperature can decrease the molecular weight and glass transition temperature in poly(methyl methacrylate) (PMMA) or poly(ethylene propylene) (PEP). Our group had reported that the PEO-lithium salt (LiBF<sub>4</sub>, LiCF<sub>3</sub>SO<sub>3</sub>) based polymer electrolyte prepared by ball milling for lithium

\* Corresponding author.

E-mail address: [kiwonkim@nongae.gsnu.ac.kr](mailto:kiwonkim@nongae.gsnu.ac.kr) (K.W. Kim).

sulfur cell showed higher ionic conductivity and good interfacial stability [7–9]. We found that ball milled PEO-base polymer electrolytes with ceramic filler (BCPE) displayed higher ionic conductivity and interfacial stability than that without ceramic fillers (BPE) [10].

In the present work, we employed differently treated PEO polymer electrolytes, stirred polymer electrolyte (SPE) and two-modified PEO polymers electrolyte (BPE and BCPE). These polymers were applied to Li/S cells, and the effects of  $\text{LiS}_n$  and lithium sulfide on the cycle characteristics were investigated.

## 2. Experimental

Poly-ethylene oxide (PEO) electrolyte was prepared by mixing PEO and  $\text{LiBF}_4$  powder. Nano- $\text{Al}_2\text{O}_3$  was added to investigate effects of ceramic filler on the electrochemical properties of a Li/S cell. These powders were blended and dissolved into acetonitrile (AcN) to make slurry. The slurry was ultrasonically dispersed for 1 h, stirred for 24 h and then ball-milled for 12 h. The ball-milled slurry was cast on a glass plate and dried in a glove box at  $60^\circ\text{C}$  for 24 h.

Sulfur slurry for cathode was prepared with elemental sulfur, carbon, PEO and AcN. The sulfur and carbon ( $<1\ \mu\text{m}$ , acetylene black, 50% compressed, Alfa. Co.) were already dried under vacuum at 90 and  $120^\circ\text{C}$  for 24 h, respectively. Here, PEO was used as a binder. The slurry was mixed by a magnetic stirrer for 24 h and then it was cast on glass plate and dried in a glove box at  $60^\circ\text{C}$  for 24 h. Lithium foil (Cyprus Foote mineral Co.) was used for anode material. The cell was assembled by stacking lithium, electrolyte and sulfur electrode in turn. Discharge and charge test were conducted at  $80^\circ\text{C}$  with constant current rate of  $0.07\ \text{mA cm}^{-2}$ . Cut-off voltage of discharge test was 1.7 V. The XRD phase analysis of sulfur electrode was carried out by a Rigaku diffractometer. (Cu-K $\alpha$  radiation) was used in all experiments and step scanner was employed at a scanning rate of  $2^\circ\ \text{min}^{-1}$ .

## 3. Results and discussion

Fig. 1 shows SEM morphologies of  $(\text{PEO})_6\text{LiBF}_4$  polymer electrolytes prepared with different methods; stirred polymer electrolyte (SPE), ball-milled polymer electrolyte (BPE) and ball-milled polymer electrolyte with  $\text{Al}_2\text{O}_3$  (BCPE). There

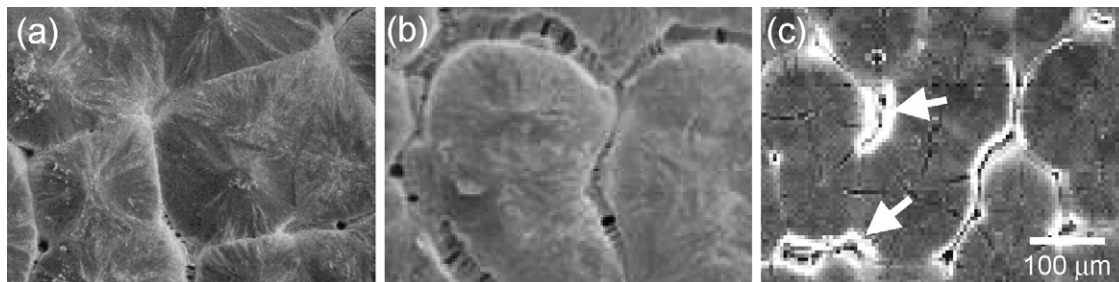


Fig. 1. SEM micrographs of  $(\text{PEO})_6\text{LiBF}_4$  polymer electrolyte prepared by three different treatments; (a) SPE, (b) BPE, and (c) BCPE. Arrows in (c) indicate  $\text{Al}_2\text{O}_3$  additive.

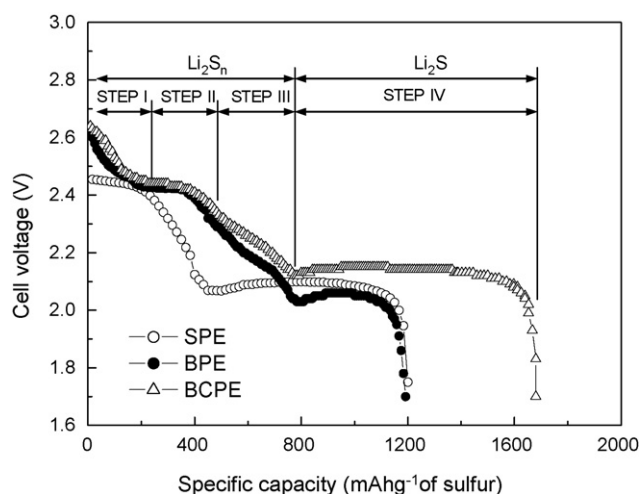


Fig. 2. First discharge profiles of Li/ $(\text{PEO})_6\text{LiBF}_4$ /S cells with discharge current rate of  $0.07\ \text{mA cm}^{-2}$  at  $80^\circ\text{C}$  for the  $(\text{PEO})_6\text{LiBF}_4$  polymer electrolyte prepared by stirring, ball milling and ball milling with  $\text{Al}_2\text{O}_3$ .

exists a grain like spherulite structure on the surface of SPE, BPE and BCPE. This is a typical morphology of a crystalline polymer with flexible chains. Morphological change of three polymer electrolytes is investigated in terms of spherulite size and gap between spherulites. The size of spherulite was measured, and the average diameter was  $200\ \mu\text{m}$  for SPE,  $250\ \mu\text{m}$  for BPE and  $180\ \mu\text{m}$  for BCPE, respectively. The size of spherulite in BPE increased by the ball milling, while the size in BCPE decreased by adding  $\text{Al}_2\text{O}_3$  particle, which acted as a nucleation site of spherulite and an obstacle of the a spherulite growth. In addition, gaps between spherulites were  $8\ \mu\text{m}$  for SPE,  $22\ \mu\text{m}$  for BPE and  $11\ \mu\text{m}$  for BCPE. PEO polymer is polymerized by binding PEO chain, the increase of binding PEO chain causes a large amount of shrinkage. Shin et al. [7] reported that the number of PEO chain was increased by ball milling. Thus, the increase of gaps in BPE is caused by the shrinkage of spherulite toward its center. Expanded pores in Fig. 1(b) resulted from the shrinkage. However, Fig. 1(c) shows that the gap between spherulite decreases and this gap is filled with  $\text{Al}_2\text{O}_3$  particles.

Fig. 2 shows the first discharge curves of Li/S cells with three different PEO electrolytes. Significant changes in the reaction step and the discharge capacity are observed with different preparations of the electrolyte.

Table 1

Reaction equation of four-step discharge for Li/S cells

Reaction equation	Theoretical capacity: step
$2\text{Li} + \text{S} \leftrightarrow \text{Li}_2\text{S}$	1672 mAh g <sup>-1</sup> -S: overall reaction
$2\text{Li} + \text{S}_8 \leftrightarrow \text{Li}_2\text{S}_8$	209 mAh g <sup>-1</sup> -S: Step I
$2\text{Li} + \text{Li}_2\text{S}_8 \leftrightarrow 2\text{Li}_2\text{S}_4$	209 mAh g <sup>-1</sup> -S: Step II
$2\text{Li} + \text{Li}_2\text{S}_4 \leftrightarrow 2\text{Li}_2\text{S}_2$ (insoluble)	418 mAh g <sup>-1</sup> -S: Step III
$2\text{Li} + \text{Li}_2\text{S}_2 \leftrightarrow 2\text{Li}_2\text{S}$ (insoluble)	836 mAh g <sup>-1</sup> -S: Step IV

Regarding to the reaction step, two steps appear in the Li/S cell using SPE (SPE cells) and four steps appear in Li/S cells with BPE cell and BCPE cells. Each reaction of BCPE cell has a clear discharge curve compared to BPE cell. In general, it is well known that two steps as shown in the SPE cell, which are caused by the formations of  $\text{LiS}_n$  and lithium sulfide ( $\text{Li}_2\text{S}$ ), appear at 2.4 and 2.0 V in the typical discharge curve of Li/S cell [1,11,12]. However, in contrast to the typical discharge behavior, when the ball-milling process was applied to prepare the PEO electrolyte in our work, fresh steps were observed at 2.65 and 2.3 V, indicating that additional reactions occurred between Li and S. The reactions that correspond to Step I and Step III in discharge curves of SPE and BCPE will be mentioned in later. It is considered that the additional reactions result from the improved ionic conductivity of PEO electrolyte. In the previous work, when the ball milling process was applied to the preparation of PEO electrolyte, ionic conductivity of SPE was  $0.5 \times 10^{-4} \text{ Scm}^{-1}$  and that of BPE was  $3 \times 10^{-4} \text{ Scm}^{-1}$  at 80 °C [7]. Thus, the electrolytes with relatively high conductivity supply sufficient Li ions to S and  $\text{LiS}_n$ , resulting in the formation of the steps at 2.65 and 2.3 V.

For the discussion, the reaction steps shown in Fig. 2 are marked as Step I, II, III and IV. Based on the theoretical capacity, it can be considered that the products formed at the each reaction are  $\text{Li}_2\text{S}_8$ ,  $\text{Li}_2\text{S}_4$ ,  $\text{Li}_2\text{S}_2$  and  $\text{Li}_2\text{S}$  and estimated reactions for the products are shown in Table 1. Experimental capacity of each reaction was about 200(I), 200(II), 400(III) and 800 mAh g<sup>-1</sup>-sulfur(IV) as shown in Fig. 2. Even though, a quantitative analysis was not performed, the calculated capacity of each reaction shows a good agreement with our results.

Regarding to the discharge capacity, the capacity is 1200 mAh g<sup>-1</sup>-sulfur for the SPE and BPE cells, while that of the BCPE cell is to 1670 mAh g<sup>-1</sup>-sulfur, approximately equal to theoretical capacity of Li/S cell. The capacity of the BPE and BCPE cell show similar value until Step II. However, difference between them is presented from Steps III to IV. The capacity of Step IV for BCPE cell was higher capacity of 470 mAh g<sup>-1</sup>-sulfur than that for BPE cell. This can be considered that the capacity difference of Step IV is caused by the amount of  $\text{LiS}_n$  dissolved and diffused into an electrolyte. According to Peled [1] and Kim [11],  $\text{LiS}_n$  is dissolved into electrolyte during discharge process. A more details of  $\text{LiS}_n$  diffusion will be described with a basis of surface observation. Thus, it is found that the discharge behavior and the discharge capacity of Li/S cells are strongly affected by the preparation process of electrolytes and an additive material.

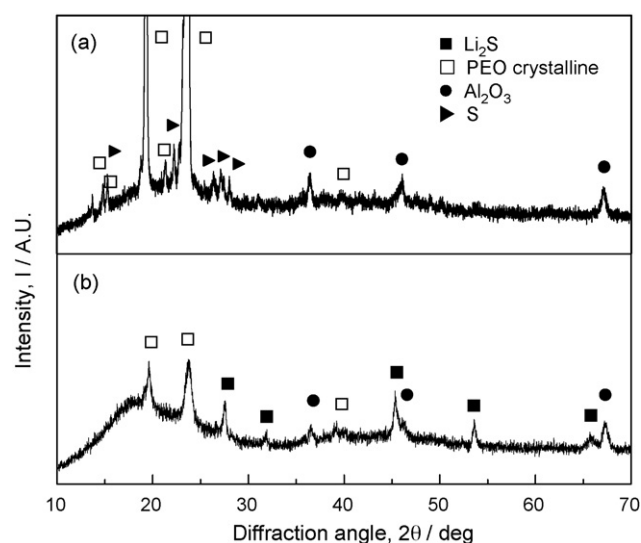


Fig. 3. XRD patterns of sulfur electrode (a) before discharge and (b) after discharge.

Fig. 3 shows the XRD patterns of sulfur composite electrode using the BCPE electrolyte before discharge and after full discharge. Before discharge, diffraction peaks of original sulfur are clearly observed together with those of PEO and  $\text{Al}_2\text{O}_3$ . After full discharge, the sulfur peaks disappeared and  $\text{Li}_2\text{S}$  peak appeared freshly. This indicates that sulfur is transformed  $\text{Li}_2\text{S}$  during discharge process and  $\text{Li}_2\text{S}$  is fully utilized for Li/S cells as shown in Fig. 2, and showing a good agreement with our estimated reaction. Additionally, we also analyzed on  $\text{LiS}_n$  formed each reaction because discharge behaviors and capacity of BPE and BCPE are closely related to the reactions of  $\text{LiS}_n$  and  $\text{Li}_2\text{S}$ . Eventually, we could not observe any peaks of products associated with Step I, II and III. In order to investigate the behavior of  $\text{LiS}_n$  between Step I and Step IV, the discharge tests at various depth of discharge (DOD) for the BPE and BCPE cells were performed as a function of calculated capacity.

Fig. 4 shows the discharge curves of BPE cell at various discharge conditions. Each discharge condition was 12.5% (200 mAh g<sup>-1</sup>-sulfur), 25% (400 mAh g<sup>-1</sup>-sulfur), 50% (800 mAh g<sup>-1</sup>-sulfur) and 100% (1670 mAh g<sup>-1</sup>-sulfur) DOD. Each DOD corresponds to the capacity of individual step from Step I to Step IV. The cycle number is described under each discharge curve. Step I appears at only first cycle in Fig. 4(a–d) and disappears at the second cycle. Step II is reversed with constant capacity until second cycle in Fig. 4(a) and (b), and disappears at third cycle. At Fig. 4(b–d), however Step III and Step IV are reversed with constant capacity until second cycle and then their capacities drastically decreased in third cycle. These results indicate that Step I and Step II are an irreversible reaction, while Step III and Step IV are partially reversible reactions.

Fig. 5 shows the discharge curves of BCPE cell at various discharge conditions. At BCPE cell, discharge behaviors of four steps are similar to those of BPE cells, while discharge capacity of Step III and Step IV is drastically increased at 50% and

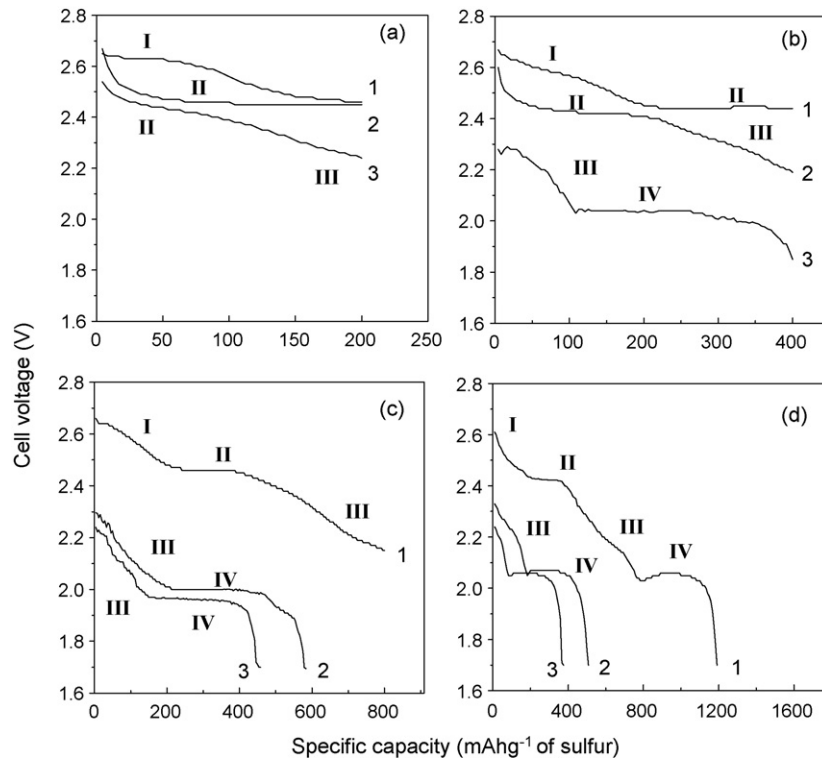


Fig. 4. Voltage profiles of (a) 200 mAh g<sup>-1</sup>-sulfur, (b) 400 mAh g<sup>-1</sup>-sulfur, (c) 800 mAh g<sup>-1</sup>-sulfur, and (d) full discharge with discharge current rate of 0.07 mA cm<sup>-2</sup> at 80 °C for Li/BPE/S cells.

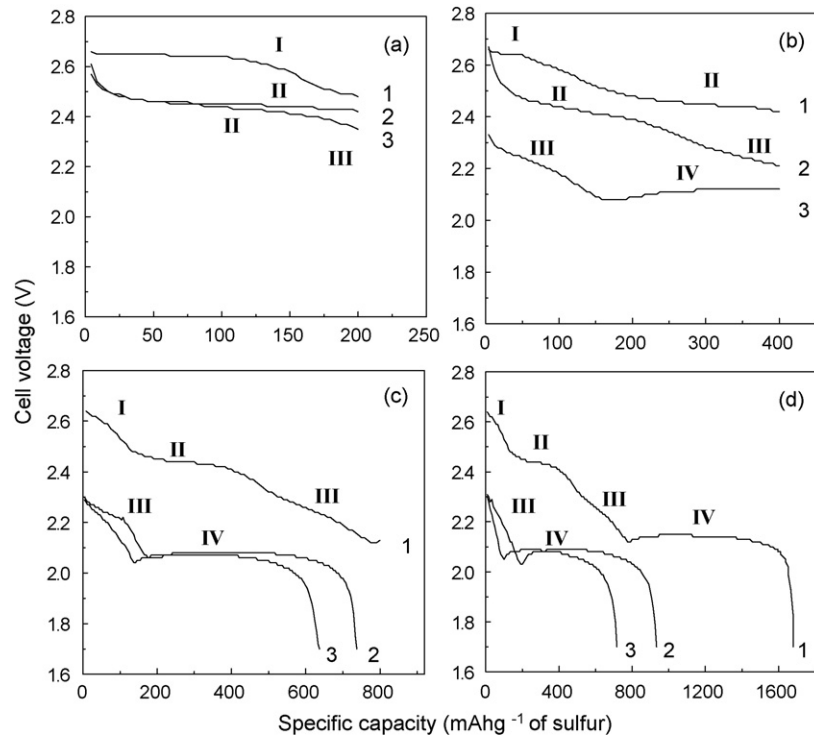


Fig. 5. Voltage profiles of (a) 200 mAh g<sup>-1</sup>-sulfur, (b) 400 mAh g<sup>-1</sup>-sulfur, (c) 800 mAh g<sup>-1</sup>-sulfur, and (d) full discharge with discharge current rate of 0.07 mA cm<sup>-2</sup> at 80 °C for Li/BCPE/S cells.

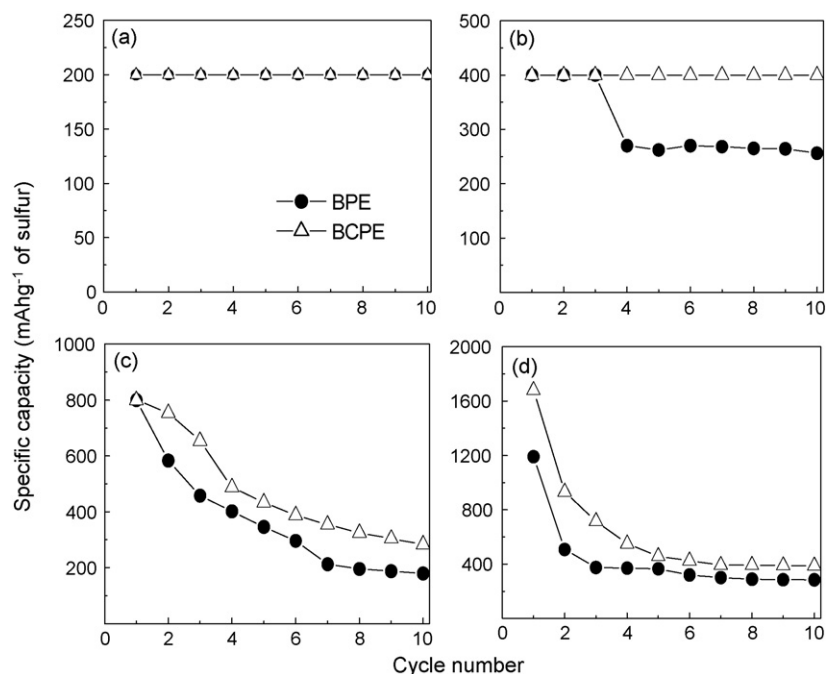


Fig. 6. Comparison of cycle performance discharged to (a) 12.5%, (b) 25%, (c) 50%, and (d) 100%DOD with discharge current rate of  $0.07 \text{ mA cm}^{-2}$  at  $80^\circ \text{C}$  for  $\text{Li}/(\text{PEO})_6\text{LiBF}_4/\text{S}$  cells.

100%DOD. This implies that a loss of  $\text{LiS}_n$  is smaller than that of BPE cell, and eventually it makes possible higher discharge capacity at consecutive Step IV discharge.

For comparison, cyclic behaviors of BPE and BCPE cells at various DOD are shown in Fig. 6. Difference in capacity is obviously observed at 25% DOD, where  $\text{Li}_2\text{S}_8$  is mainly produced. BPE shows a loss of discharge capacity at fourth cycle, while the capacity of BCPE cell keeps constant. When in considering the loss of capacity in BPE cell, once a reaction of Step I occurs ( $2\text{Li} + \text{S}_8 \leftrightarrow \text{Li}_2\text{S}_8$ ),  $\text{Li}_2\text{S}_8$  is not decomposed into the original sulfur ( $\text{S}_8$ ) and the metallic Li. Here,  $\text{Li}_2\text{S}_8$  was gradually dissolved in an electrolyte and diffused to the surface of cathode by concentration gradient. This effect would be slight at Step I but accelerated with progress of step. Moreover, the microstructure of BPE with a wide gap between spherulites helps the diffusion of  $\text{LiS}_n$ . Eventually, substantial amount of  $\text{LiS}_n$  is transferred to the cathode surface and then dissolved into the electrolyte. The loss of  $\text{LiS}_n$  causes the decrease in the capacity of Step II and Step III during the cycling.

On the other hand, in the case of BCPE cell, the dissolution of  $\text{LiS}_n$  into electrolyte can be restrained by the addition of  $\text{Al}_2\text{O}_3$  having strong adsorption. Smaller loss of  $\text{LiS}_n$  in case of BCPE cell could be considered as related to the adsorption effect by nano-sized  $\text{Al}_2\text{O}_3$  particles. The steep decrease in second cycle is due to irreversibility of Step I and Step II. These curves show that BCPE has better cycle performance than BPE cell.

#### 4. Conclusions

In this study, we have presented electrochemical properties of sulfur composite electrode using stirred polymer electrolyte

(SPE), ball milled polymer electrolyte (BPE) and ball milled polymer electrolyte with  $\text{Al}_2\text{O}_3$  (BCPE). From the results of discharge profile, the number of step was two for the SPE cells and four for the BPE and BCPE cells. Initial discharge capacity was improved by the ball milling and the addition of  $\text{Al}_2\text{O}_3$  to  $(\text{PEO})_6\text{LiBF}_4$  polymer electrolyte. Discharge profile for the BPE and BCPE cells showed that Steps I and II was rapidly faded and these reaction is irreversible. Cyclic performance for BCPE cells was improved than that for BPE cell at Step IV, particularly at 25%DOD cycles. These improvements of cell performance were attributed to the stability of 2.1 V plateau, thus  $\text{Al}_2\text{O}_3$  filler stabilized formation of  $\text{Li}_2\text{S}$  and improved utilization of sulfur.

#### Acknowledgement

This work was supported by University IT Research Center Project from Ministry of Information and Communication.

#### References

- [1] H. Yamin, A. Gorenshtein, J. Penciner, Y. Sternberg, E. Peled, J. Electrochem. Soc. 135 (1988) 1045–1048.
- [2] A. Gorkovenko, US patent No. 6,210,831 B1 (2001).
- [3] F. Croce, G.B. Appetecchi, L. Persi, B. Scrosati, Nature 394 (1998) 456–458.
- [4] F. Croce, R. Curini, A. Martinelli, L. Persi, F. Ronci, B. Scrosati, J. Phys. Chem. B 103 (1999) 10632–10638.
- [5] W. Krawice, L.G. Scanlon Jr., J.P. fellner, R.A. Vaia, S. Vasudevan, J. Power Sources 54 (1995) 310–315.
- [6] A.P. Smith, J.S. Shay, R.J. Spontak, C.M. Balik, H. Ade, S.D. Smith, C.C. Koch, Polymer 41 (2000) 6238–6271.

- [7] J.H. Shin, Y.T. Lim, K.W. Kim, H.J. Ahn, J.H. Ahn, *J. Power Sources* 107 (2002) 103–109.
- [8] J.H. Shin, S.S. Jung, K.W. Kim, H.J. Ahn, *J. Mater. Sci.: Mater. Electron.* 13 (2002) 727–733.
- [9] J.H. Shin, B.S. Jung, S.S. Jeong, K.W. Kim, H.J. Ahn, K.K. Cho, J.H. Ahn, *Met. Mater.* 1 (2) (2004) 177–183.
- [10] S.S. Jeong, Y.T. Lim, B.S. Jung, K.W. Kim, *Mater. Sci. Forum* 486–487 (2005) 594–597.
- [11] S.E. Cheon, K.S. Ko, J.H. Cho, S.W. Kim, E.Y. Chin, H.T. Kim, *J. Electrochem. Soc.* 150 (2003) 800–805.
- [12] M.S. Song, S.C. Han, H.S. Kim, J.H. Kim, K.T. Kim, Y.M. Kang, H.J. Ahn, S.X. Dou, J.Y. Lee, *J. Electrochem. Soc.* 151 (2004) 791–795.